Available online at www.sciencedirect.com

SCIENCE DIRECT®

Earth and Planetary Science Letters 222 (2004) 741–750

EPSL

www.elsevier.com/locate/epsl

The Younger Dryas—an intrinsic feature of late Pleistocene climate change at millennial timescales

Adriana Sima*, André Paul[1], Michael Schulz[2]

Department of Geosciences, University of Bremen, D-28334 Bremen, Germany

Received 25 July 2003; received in revised form 26 January 2004; accepted 23 March 2004

Abstract

A box model of the North Atlantic Ocean exhibits self-sustained oscillations of the large-scale ocean circulation, which are reminiscent of Dansgaard–Oeschger (DO)-style oscillations. The freshwater forcing of this ocean model depends on mean climate state, represented by global ice volume. This is computed by a one-dimensional ice-sheet model, subject to changes in high-latitude northern hemisphere summer insolation. At low/large ice volume, the ocean–ice system stays in a permanent interstadial/stadial mode. Millennial scale DO-style oscillations result at intermediate ice-volume values, which thus define a ''DO window''. During an interglacial-to-glacial transition, this DO window is crossed sufficiently slow to allow for sustained DO-style oscillations to develop. In contrast, during a glacial termination, the system moves relatively rapid through the DO window, resulting in an intermittent re-appearance of DO-style oscillations, which resemble the sequence of events surrounding the Younger Dryas (YD). When forced with modeled ice-volume evolution over the last 800 thousand years, our model predicts Younger-Dryas-type cooling events for each major glacial termination. Accordingly, the Younger Dryas does not appear to be a one-time event.

Keywords: deglaciation; abrupt climate change; deep-decoupling oscillation; ice-sheet model

1. Introduction

The Younger-Dryas (YD) cold spell is one of the most prominent abrupt climate change events in the past and a key feature of the last glacial termination. It is an intermittent, ~1300-year long return to almost glacial conditions within a general warming trend. At least in the Northern Hemisphere, the last deglaciation appears as a sequence of three main intervals: the Bølling/Allerød warm period (approximately between 14,700 and 12,900 years BP), the YD cold phase (~12,900–11,600 years BP) and the warm Preboreal (after ~11,600 years BP) (all dates refer to the Greenland ice core GISP2 chronology; [1]). Although the YD event mainly affected the Northern Hemisphere, it was of global significance (e.g. [2]).

Different hypotheses have been suggested to explain the YD ([2] for a summary). The majority of ideas favor the ocean as a crucial element for

* Corresponding author. Tel.: +49-421-218-7188; fax: +49-421-218-7040.

E-mail addresses: sima@palmod.uni-bremen.de (A. Sima), apau@palmod.uni-bremen.de (A. Paul), mschulz@palmod.uni-bremen.de (M. Schulz).

[1] Tel.: +49-421-218-7189; fax: +49-421-218-7040.

[2] Tel.: +49-421-218-7136; fax: +49-421-218-7040.

0012-821X/$ - see front matter © 2004 Elsevier B.V. All rights reserved.
doi:10.1016/j.epsl.2004.03.026

generating the YD. In this view, differential meltwater input into the North Atlantic is hold responsible for slowing down the Atlantic Ocean meridional overturning circulation, either by re-routing Lake Agassiz water to the St. Lawrence River [3] or by a delayed response to the so-called meltwater pulse 1A (MWP-1A; e.g. [4,5]), which commenced approximately 1800 years prior to the onset of the YD and culminated during the Bølling warm period [6,7]. Berger and Jansen [8] proposed a variation on this general theme in that they consider the Bølling/Allerød warm period as an intermittent state, triggered by the wasting of marine-based ice sheets around the North Atlantic Ocean, and the YD as a mere return to glacial conditions.

The rerouting hypothesis [3] faces the difficulty that the thermohaline circulation in the North Atlantic prior to the onset of the YD was relatively strong and probably harder to destabilize than originally suggested by coarse resolution models [9]. When assuming a meltwater-induced triggering of the YD, the immediate problem is to explain the time lag between MWP-1A and the onset of the YD. Furthermore, the northern hemisphere origin of MWP-1A is still questionable (e.g. [10]), making this meltwater input as trigger for the YD even more unlikely. From experiments with an Earth system model of intermediate complexity, Crucifix and Berger [11] also concluded that there was probably no direct link between MWP-1A and the initiation of the YD.

Based on the methane record in the Antarctic Vostok ice core for the past 420 kyr [12], Broecker [13] argued that the YD appeared to be a one-time event and not a general feature of glacial terminations. However, the time resolution of the Vostok methane record is on the order of 1000–2000 years before the penultimate interglacial [12] and therefore prevents any unambiguous detection of YD-type events.

In contrast to the supposition of a one-time event, paleoceanographic reconstructions show some evidence for cold events similar to the YD during five terminations preceding Termination I [14]. More recently, Lototskaya and Ganssen [15] identified a ‘‘Termination II pause’’ which separated the penultimate deglaciation into two steps. Sea-level reconstructions from coral data [16] even suggest a return to colder conditions associated with a regrowth of continental ice during Termination II. Thus, the YD may not be a singular event, but an intrinsic feature of glacial terminations.

Here we propose an alternative mechanism to account for the YD and similar earlier events, which does not depend on meltwater input into the North Atlantic. We approach the YD from the Northern Hemisphere point of view and elaborate on an idea put forth by Schulz et al. ([17], hereafter SPT). We consider the trigger of the YD to reside in the ocean, and envision the YD cold phase as part of one cycle of a so-called deep-decoupling oscillation of the Atlantic Ocean meridional overturning circulation. Such a cycle may occur during any termination when the mean climate passes through an intermediate state, between glacial maximum and interglacial.

Deep-decoupling oscillations [18–21] can be caused by a continuous freshening of the North Atlantic Ocean, which leads to the development of a polar halocline and eventually suppresses the formation of North Atlantic Deep Water. During this ‘‘deep-decoupled phase’’, the meridional circulation and oceanic heat transport are reduced. The subsequent import of heat and salt by advection and diffusion weakens the stratification and finally destroys the polar halocline. The renewal of convection in high latitudes marks the onset of a ‘‘deep-coupled phase’’, with active deep-water formation and vigorous meridional overturning circulation and heat transport. The reestablishment of the halocline then completes a ‘‘deep-decoupling oscillation’’. From the abruptness of the transitions, deep-decoupling oscillations are reminiscent of the millennial-scale climate variability documented in the Greenland ice cores [22]. Following [19], we interpret the deep-decoupled phases as Dansgaard–Oeschger (DO)-stadials and the deep-coupled phases as DO-interstadials.

2. Methods

To study deep-decoupling oscillations of the meridional overturning circulation in relation to DO oscillations, we use a combination of ice-sheet and ocean modeling. With the help of a one-dimensional ice-sheet model, we generate a history of glaciation, which, in turn, is used to modulate the low-to-high-latitude freshwater forcing in an ocean box model. Finally, we compare the model results to a reconstruc-

tion of global sea level and to the oxygen-isotope composition of Greenland ice.

2.1. Ice-sheet model

The one-dimensional coupled ice-sheet-bedrock model (after [23,24]) considers only the Laurentide ice sheet, which dominated ice-volume variations during the late Pleistocene (cf. [25]). Ice thickness and bedrock elevation are computed as functions of latitude and time along a typical flow line through the ice sheet, such that a north–south profile is approximated.

Ice flow is described by a vertically integrated continuity equation for ice thickness:

$$\frac{\partial h_i}{\partial t} = -\frac{\partial(\bar{U}h_i)}{\partial x} + B - C, \quad (1)$$

where h_i is ice thickness and $\bar{U}$ is the vertically averaged horizontal velocity (see Table 1 for symbols and parameter values). The first term on the right-hand side represents internal ice shear or basal sliding at the ice-bed interface. We compute $\bar{U}$ as:

$$\bar{U} = Ah_i^{n+1}\left|\frac{\partial(h_i+h_b)}{\partial x}\right|^{n-1}\frac{\partial(h_i+h_b)}{\partial x},$$

where h_b is the bedrock elevation above sea level. Net annual mass balance B on the ice surface is derived using the equilibrium-line concept, as follows [26,23]:

$$B = \begin{cases} a(h_i+h_b-h_{equ}) - b(h_i+h_b-h_{equ})^2 & \text{if } h_i+h_b-h_{equ} \le 1500\ m \\ 0.56 & \text{if } h_i+h_b-h_{equ} > 1500\ m \end{cases} \times \text{m year}^{-1}.$$

The equilibrium-line elevation is assumed to depend linearly on latitude and insolation variations:

$$h_{equ} = h_{equ}^0 + s_{equ}x + k_{ins}\Delta Q$$

where ΔQ is the difference in the caloric summer insolation at 55°N [27] from that of the present. Fourier coefficients for computing the Earth's orbital elements are taken from Berger [28]. The term C in Eq. (1) represents catastrophic calving. It is set to 20 m yr^{-1} at any grid point of the ice sheet if its base is below sea level (h_b<0) and if the grid point or one of its neighbouring points has floating ice ($\rho_i h_i$<$-\rho_w h_b$).

Table 1
Parameters of the one-dimensional ice-sheet model

Symbol	Description	Value	Units
x	north–south distance	independent variable	m
t	time	independent variable	yr
$h_i(x,t)$	ice-sheet thickness	prognostic variable	m
$h_b(x,t)$	bedrock elevation above sea level	prognostic variable	m
$h_b^{eq}(x,t)$	equilibrium bedrock elevation above sea level	500 southward of 70°N, −500 northward of 74°N, linear ramp between 70° and 74°N	m
h_{equ}^0	altitude of equilibrium line at 70°N	550	m
s_{equ}	slope of equilibrium line	0.001	
k_{ins}	proportionality factor for equilibrium-line elevation	35.1	m W^{-1} m^2
B	mass balance on ice surface	prescribed (see text)	m yr^{-1}
C	calving rate	20 if 'floating' (see text)	m yr^{-1}
A	ice rheology coefficient	5.77×10^{-4}	m^{-3} yr^{-1}
n	ice rheology exponent	3	
a	coefficient in mass balance	0.81×10^{-3}	yr^{-1}
b	coefficient in mass balance	0.30×10^{-6}	m^{-1} yr^{-1}
τ	timescale of bedrock relaxation	5000	yr
ρ_i	ice density	910	kg m^{-3}
ρ_b	bedrock density	2390	kg m^{-3}

The calving instability does not introduce ice-age terminations, but amplifies them [23].

Bedrock adjustment is computed from a "local lithosphere-relaxed asthenosphere" model [29] with a characteristic time constant τ:

$$\frac{\partial h_b}{\partial t} = \frac{1}{\tau}\left[h_b^{eq} - h_b - \frac{\rho_i h_i}{\rho_b}\right],$$

where h_b is the bedrock elevation above sea level, h_b^{eq} is the equilibrium bedrock elevation above sea level, ρ_i the ice density and ρ_b the bedrock density. In the

direction normal to the flow line, no ice-sheet dynamics is computed, but a perfectly plastic profile symmetric to the ice-sheet crest is assumed [30]. This enables us to compute a three-dimensional ice-volume from the two-dimensional cross-sectional area of the ice sheet.

Ice volume is converted to sea level taking into account the total sea surface and the ratio of seawater and ice densities. Thus, we equate 1 m of sea level with 4.091×10^{14} m^3 of ice.

The resulting ice equivalent sea-level variations are multiplied by a factor of 1.6 to match the sea level at the Last Glacial Maximum (LGM) [31]. In this way, we account for the continental ice not represented in our model (e.g. the Eurasian ice sheet). In accordance with Peltier [25], a ~60% contribution of the Laurentide ice sheet to the total sea level at LGM is therefore assumed.

2.2. Ocean model

The three-box model of the North Atlantic Ocean (Fig. 1) is based on Winton [19]. We use the same parameters as in SPT. The height of the two surface boxes is h=100 m and that of the deep box is H=1000 m. The boundary between low- and high-latitude surface boxes is associated with the subpolar front in the Atlantic Ocean. The northern box represents regions in which deep convection and deep-water formation take place (i.e. the subpolar North Atlantic and Norwegian–Greenland Seas at present). All the boxes have a longitudinal extent of 60°. Temperatures

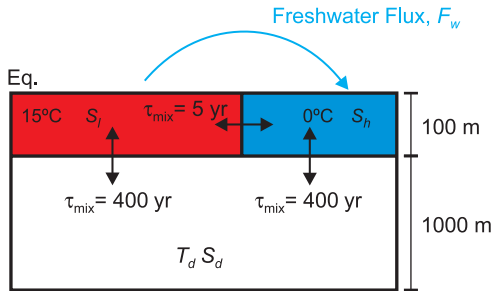

Fig. 1. Three-box model of the North Atlantic Ocean (after [19]). Each box is characterized by temperature (T) and salinity (S). Subscripts 'l' and 'h' denote low- and high-latitude boxes and 'd' the deep box. M_{ij} is the mixing between boxes i and j. F_w is the low-to-high-latitude freshwater flux (see text for further details).

in the surface boxes are constant with T_l=15 °C and T_h=0 °C. The temperature in deep box (T_d) and salinities (S) in all boxes are computed. Mixing M_{ij} between boxes i and j occurs at timescale τ_{ij} such that $M_{ij}=d_{ij}/\tau_{ij}$, where d_{ij} is the exchange-area-weighted distance between box centers ($\tau_{ld}=\tau_{hd}$=400 yrs and τ_{lh}=5 yrs). Using a quadratic equation of state, M_{hd} is increased by a factor C_h=10 if the high-latitude water column is gravitationally unstable; else C_h=3 is adopted to account for partial shutdown of multiple convection sites.

As in SPT, we assume a linear relationship between the high-latitude net surface freshwater flux (F_w) and ice-equivalent sea level (Sl): $F_w=a+b\times$Sl, with a= 0.5015 m yr^{-1} and $b=-4.5\times10^{-3}$ yr^{-1}. We stress that sea level is envisaged here as a measure of the mean climate state. Our hypothesis that the high-latitude net surface freshwater flux is enhanced during glacials is based on the following factors:

1. Reduction of evaporation.
2. Southward shift of the storm-track.
3. Melting of sea ice.
4. Melting of icebergs in regions of seasonal sea-ice cover.
5. Increased runoff from European rivers, which carry meltwater from snow and from the southern margin of the ice sheets.

All these processes are directly or indirectly related to the presence of large ice sheets in the Northern Hemisphere and have been quantified for the LGM. Factors 1 to 3 were made responsible for the increase in freshwater flux in the latitudinal belt between 40° and 60°N during the LGM [32]. Schmittner et al. [33] found that it was mainly factor (1) that caused the reduced thermohaline circulation in their simulation of the LGM. Factors 4 and 5 were inferred by Duplessy et al. [34] from the distribution of oxygen isotopes of planktonic foraminifera in the northern North Atlantic Ocean, especially in the Bay of Biscay and the Nordic Seas. Melting of icebergs and ice sheets (cf. factors 4 and 5) is usually not taken into account in climate models. We assume that the effect of the enhanced high-latitude freshwater flux on the buoyancy flux outweighs the effect of the high-latitude cooling, leading to reduced deep-water formation in the North Atlantic. Since the focus of this study is on the

generation of YD-type events, the parameterization of Heinrich events employed by SPT is not used here.

3. Results

The modeled ice-equivalent sea level is shown in Fig. 2. It exhibits glacial–interglacial cycles of about 100-kyr period, characterized by slow build-up and rapid decay of ice. The state of the ocean box model is determined by the modeled variations of the ice volume via the relationship between Sl and F_w. At low values of the freshwater forcing (F_w), the model stays in a permanent interstadial phase, while high values of F_w result in a continuous stadial phase (Fig. 3, see also SPT). For intermediate values of F_w, the model exhibits free oscillations which are reminiscent of DO-cycles (Fig. 4). The "strong"-convection phase represents a DO interstadial and the "weak"-convection phase characterizes the DO stadial mode. The latter mode is also considered as surrogate for the LGM state in our model. Although this assumption is in accordance with the common interpretation of paleoceanographic proxy data (summarized in [35]), these data may actually be insufficient to constrain the LGM circulation [36]. DO-style oscillations occur for F_w values between 0.704 and 0.875 m yr^{-1}. This "DO window" (Fig. 3) corresponds to a sea-level range of −45 to −83 m, consistent with the earlier findings [37,38]. Within the DO window, the duration of the stadials increases with rising F_w (SPT).

When forced with the modeled ice-volume evolution, the predicted climate oscillations during the last glacial period show structural similarities with the reconstructed climate fluctuations (Fig. 5). Before ~75 kyr BP, the ice-equivalent sea level is above the upper limit of the DO window, so the ice–ocean system stays in the interstadial (warm) mode. Between ~75 and 70 kyr BP, sea level slowly crosses the DO window, giving rise to a sequence of three stadial–interstadial oscillations. Between ~70 and 60 kyr BP, sea level drops below the lower limit of the DO

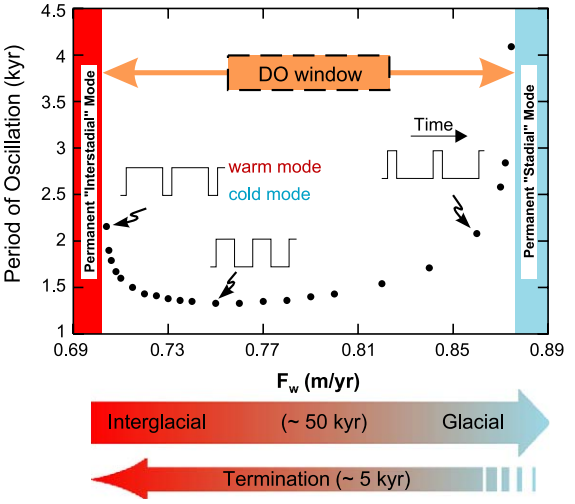

Fig. 3. Period of the oscillation in the ocean model as function of freshwater flux F_w (dots). Ratio between durations of "warm" and "cold" phases decreases with increasing F_w, as indicated by square waves (not to scale). The F_w range in which oscillations occur defines the DO window. It is slowly crossed during the transition from interglacial to glacial conditions, and more rapidly during glacial terminations.

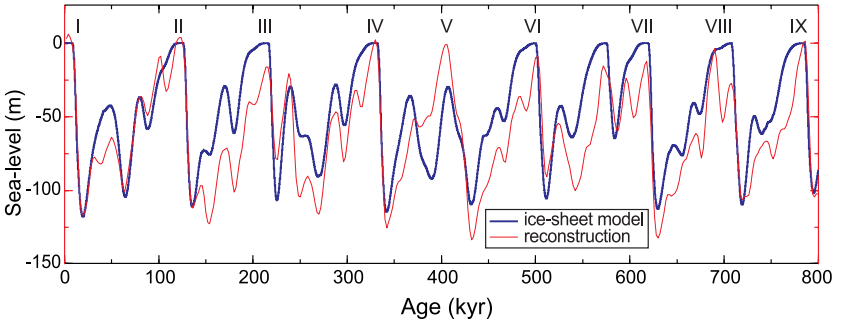

Fig. 2. Modeled ice equivalent sea-level (thick line) and sea-level reconstruction of Berger et al. ([31], thin line). A linear trend was subtracted from the reconstructed sea level to account for a long-term warming trend affecting the underlying oxygen isotope data [31]. Roman numerals denote terminations.

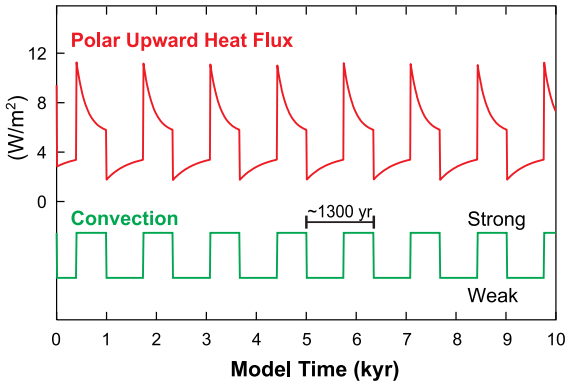

Fig. 4. Free deep-decoupling oscillation in the ocean box model for a constant freshwater flux of 0.75 m/yr.

window, so that DO-style oscillations cannot occur anymore and the system enters a permanent stadial state. At about 60 kyr BP, sea level returns into the DO-window and a more than 30-kyr-long oscillation sequence develops, only briefly interrupted around ~48 kyr BP. This interruption gives the impression of a very long interstadial, in close resemblance with the proxy data. After ~27 kyr BP, the ice volume becomes again too large to allow DO-style oscillations to develop and the system enters once again the permanent cold state. At ~18 kyr BP, the last deglaciation begins. During this glacial termination, the DO window is crossed within ~2.5 kyr, so that a single DO-style oscillation cycle occurs. This results in a succession of events similar to the Bølling/Allerød–YD–Preboreal sequence. At about 12 kyr BP, with the sea level reaching the upper limit of the DO window, the model marks the entering of a permanent warm state, corresponding to the Holocene.

The same model setup, when applied to the entire late Pleistocene, predicts YD-type events during each of the nine major terminations (Fig. 6). If, during a glacial termination, the DO window is crossed within a time interval comparable to the period of the deep-decoupling oscillation, only a single cycle will occur. Accordingly, the deglaciation proceeds in two warming steps, separated by one cold YD-style cooling event. In contrast, if the DO window is crossed within a longer time interval, more than one oscillation can develop.

Our model setup allows for two- and three-step terminations, including one or two YD-style cooling events. Terminations I, II, IV and VII fall in the first category (DO window-crossing time of 1.9–2.2 kyr) and Terminations III, VI, VIII and IX in the second (DO window-crossing time of 2.4–3.2 kyr) (Fig. 6).

An interesting situation arises for Termination V, which is known to be associated with weak orbital forcing [39]. Correspondingly, the DO window is crossed extremely slow (12.5 kyr in our simulation; Fig. 6), leading to a long sequence of DO-style oscillations. Indeed, a sequence of three benthic $\delta^{13}C$ minima, each indicating a time interval with reduced deep-water production in the North Atlantic Ocean, was found by Poli et al. [40] during this termination.

4. Discussion

Modeled ice-equivalent sea-level variations are in good agreement with the sea-level reconstruction of Berger et al. ([31]; Fig. 2). In particular, the ice-sheet model realistically simulates the 100-kyr cycles, which dominated the late Pleistocene (cf. [23]). We have chosen to compare the ice-model derived sea level to the Berger et al. [31] reconstruction since it contains only variability at orbital timescales (as does the model) and is sufficiently long to evaluate the model performance over the entire late Pleistocene.

Berger et al. [31] adopted a value of −117 m for sea level at the LGM in their reconstruction. More recent estimates are slightly lower and amount to about −125 m (e.g. [41,42]). However, choosing a different value for the sea level at LGM would only lead to different scaling parameters in the F_w–Sl relationship, but would not change the essence of our results.

The calving mechanism embodied in Eq. (1) yields the typical sawtooth shape with nine complete deglaciations during the past 800 kyr. During calving episodes, the simulated meltwater discharge reaches values up to 0.2 Sv. Because we aim at generating YD-type events independent of deglaciation meltwater input (see Introduction), this additional freshwater flux is not taken into account in computing F_w.

Compared to the reconstruction, the phasing and relative amplitude of the modeled sea-level is remarkably good over the whole investigated period. An exception is Marine Isotope Stage 11 (423–362 kyr BP); our model fails to reproduce a full deglaciation in this interval, mainly due to the weakness of the inso-

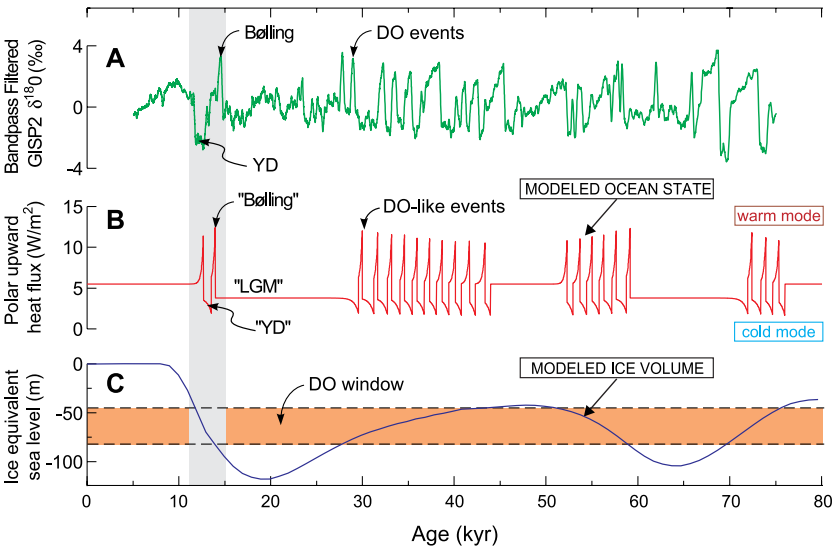

Fig. 5. Modeled climate events during the last glacial period. (A) GISP2 oxygen-isotope record, which largely reflects air-temperature above Greenland [22], band-pass filtered (STP). (B) Upward heat flux at high latitudes. (C) Modeled ice-equivalent sea level. Note that, due to the inertia of the climate system, overshoots in heat flux do not necessarily reflect similar anomalies in temperature.

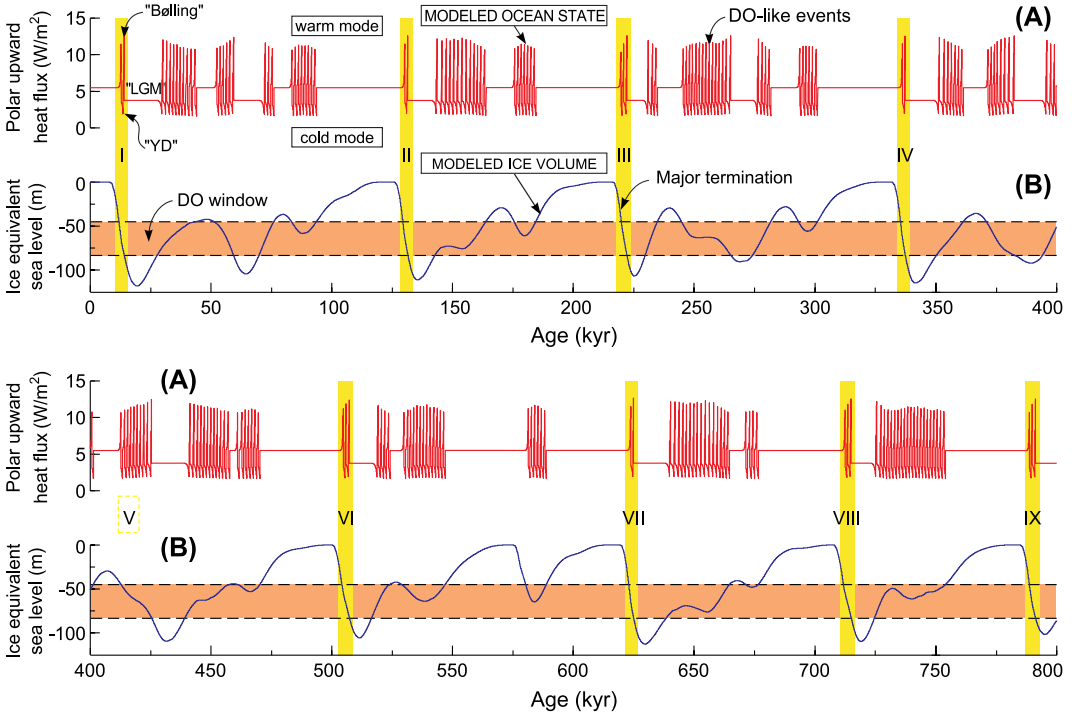

Fig. 6. Modeled climate oscillations during the past 800 kyr. (A) Upward heat flux at high latitudes. (B) Ice-equivalent sea level. Vertical bars mark glacial terminations and horizontal bar depicts DO window. Younger Dryas-type cooling events occur during all deglaciations.

lation forcing (the ''stage 11 problem'', [39]). With the same kind of model, Pollard [23] succeeded in reproducing a strong transition from isotope stages 11 to 12. In that study, a diffusive method was chosen for the asthenospheric treatment. However, there exist serious problems with this approach (e.g. the characteristic response time increases with the size of the load, in contradiction to results from a more sophisticated full-Earth model), hence, we employed the relaxed asthenosphere method, which seems preferable [29].

The appearance of the DO-style climate oscillations depends on the interaction between the period of the free oscillations and the timescale at which the mean climate (as measured by ice-volume equivalent sea level), and hence, F_w, changes. During an interglacial-to-glacial transition, the DO window is crossed within $\sim$50 kyr, which is sufficiently slow to allow sustained DO-style oscillations to develop. In contrast, during a glacial termination, the system moves relatively rapid (few kyr) through the DO window. This results in an intermittent re-appearance of DO-style oscillations, including one or two YD-type cooling events. A better fit of the timing of modeled oscillations to the proxy data during the last glacial period (Fig. 5) could possibly be achieved by choosing a different relationship between F_w and mean climate state, as measured by Sl. However, we consider such fine tuning as unwarranted within our conceptual model framework, which aims at qualitative agreement between simulation and data. The assumed linear relationship between mean climate and high-latitude freshwater flux gave a sequence of events in accordance with the paleoclimate record. We note, however, that deep-decoupling oscillations could also be induced by glacial cooling: Winton [43] showed that an ocean model can exhibit oscillatory behavior within a certain range of global mean temperature, even if freshwater forcing is held constant. Accordingly, there is possibly a DO window in temperature as well as in freshwater flux, resulting in a two-dimensional region in parameter space. This might influence a particular termination, but would not alter our general finding that the ocean–ice system intermittently oscillates as it rapidly passes through a DO window during glacial terminations.

The proposed mechanism is not mutually exclusive with meltwater-related scenarios. In fact, rerouting of meltwater from the Mississippi River drainage to the Hudson or St. Lawrence Rivers [3] may amplify the deep-decoupling oscillations during deglaciations.

5. Conclusions

Based on an idealized, prescribed ice-volume evolution, Schulz et al. [17] suggested that the Younger-Dryas event results from an intermittent re-start of self-sustained oscillations of the large-scale oceanic circulation. Instead of prescribed ice-volume variations, we use a modeled ice-volume history generated by a one-dimensional coupled ice-sheet-bedrock model, which yields a reasonable representation of the 100-kyr cycles that dominated the late Pleistocene. Considering the major glacial terminations during the past 800 kyr, the Younger-Dryas cold phase appears not as a one-time event or an ''accident'' of the last termination. On the contrary, Younger Dryas-type events seem to be an intrinsic feature of climate change during glacial–interglacial cycles. They can be conceived as Dansgaard–Oeschger stadials which are part of short Dansgaard–Oeschger oscillation sequences. Such a sequence may occur during any deglaciation, when the mean climate returns to an intermediate state and rapidly crosses the parameter range in which DO-oscillations are possible. Depending on how fast the deglaciation process develops, a glacial termination can occur in two or three steps separated by one or two YD-type cold phases.

Acknowledgements

We greatly appreciate the thorough and constructive comments by D. Paillard, an anonymous reviewer and the editor. This work was supported by the DFG within the European Graduate College ''Proxies in Earth History''. ***[BOYLE]***

References

[1] R.B. Alley, D.A. Meese, C.A. Shuman, A.J. Gow, K.C. Taylor, P.M. Grootes, J.W.C. White, M. Ram, E.D. Waddington, P.A. Zielinski, G.A. Zielinski, Abrupt accumulation increase at the Younger Dryas termination in the GISP2 ice core, Nature 362 (1993) 527–529.

[2] R.B. Alley, P.U. Clark, The deglaciation of the northern hemisphere: a global perspective, Annu. Rev. Earth Planet. Sci. 27 (1999) 149–182.
[3] P.U. Clark, S.J. Marshall, G.K.C. Clarke, S.W. Hostetler, J.M. Licciardi, J.T. Teller, Freshwater forcing of abrupt climate change during the last glaciation, Science 293 (2001) 283–287.
[4] A.F. Fanning, A.J. Weaver, Temporal–geographical meltwater influences on the North Atlantic Conveyor: implications for the younger dryas, Paleoceanography 12 (1997) 307–320.
[5] K. Sakai, W.R. Peltier, Deglaciation-induced climate variability: an explicit model of the glacial–interglacial transition that simulates both the Bolling/Allerod and Younger-Dryas events, J. Met. Soc. Jpn. 76 (1998) 1029–1044.
[6] R.G. Fairbanks, C.D. Charles, J.D. Wright, Origin of global meltwater pulses, in: R.E. Taylor, A. Long, R.S. Kra (Eds.), Radiocarbon After Four Decades, Springer-Verlag, New York, 1992, pp. 473–500.
[7] M. Kienast, T.J.J. Hanebuth, C. Pelejero, S. Steinke, Synchroneity of meltwater pulse 1a and the Bølling warming: new evidence from the South China Sea, Geology 31 (2003) 67–70.
[8] W.H. Berger, E. Jansen, Younger Dryas episode: ice collapse and super-fjord heat pump, in: S.R. Troelstra, J.E. van Hinte, G.M. Ganssen (Eds.), The Younger Dryas, R. Netherlands Acad. of Arts and Sci., Amsterdam, 1995, pp. 61–105.
[9] G. Lohmann, M. Schulz, Reconciling Bølling warmth with peak deglacial meltwater discharge, Paleoceanography 15 (2000) 537–540.
[10] P.U. Clark, J.X. Mitrovica, G.A. Milne, M.E. Tamisiea, Sea-level fingerprinting as a direct test for the source of global meltwater pulse IA, Science 295 (2002) 2438–2441.
[11] M. Crucifix, A. Berger, Simulation of ocean–ice sheet interactions during the last deglaciation, Paleoceanography 17 (2002) doi:10.1029/2001PA000702.
[12] J.-R. Petit, J. Jouzel, D. Raynaud, N.I. Barkov, J.-M. Barnola, I. Basile, J. Chappellaz, M.E. Davis, G. Delaygue, M. Delmotte, V.M. Kotlyakov, M. Legrand, V.Y. Lipenkov, C. Pépin, L. Pépin, C. Ritz, E. Saltzman, M. Stievenard, Climate and atmospheric history of the past 420,000 years from the Vostok ice core, Antarctica, Nature 399 (1999) 429–436.
[13] W.S. Broecker, Does the trigger for abrupt climate change reside in the ocean, or in the atmosphere? Science 300 (2003) 1519–1522.
[14] M. Sarnthein, R. Tiedemann, Younger Dryas-style cooling events at glacial terminations I–VI at ODP Site 658; associated benthic $\delta^{13}C$ anomalies constrain meltwater hypothesis, Paleoceanography 5 (1990) 1041–1055.
[15] A. Lototskaya, G.M. Ganssen, The structure of Termination II (penultimate deglaciation and Eemian) in the North Atlantic, Quat. Sci. Rev. 18 (1999) 1641–1654.
[16] C.D. Gallup, H. Cheng, F.W. Taylor, R.L. Edwards, Direct determination of the timing of sea level change during termination II, Science 295 (2002) 310–313.
[17] M. Schulz, A. Paul, A. Timmermann, Relaxation oscillators in concert: a framework for climate change at millennial timescales during the late Pleistocene, Geophys. Res. Lett. 29 (24) (2002) doi:10.1029/2002GL016144.
[18] L.D.D. Harvey, A two-dimensional ocean model for long-term climatic simulations: stability and coupling to atmospheric and sea ice models, J. Geophys. Res. 97 (1992) 9435–9453.
[19] M. Winton, Deep decoupling oscillations of the oceanic thermohaline circulation, in: W.R. Peltier (Ed.), Ice in the Climate System, Springer Verlag, Berlin, 1993, pp. 417–432.
[20] A. Oka, H. Hasumi, N. Suginohara, Stabilization of thermohaline circulation by wind-driven and vertical diffusive salt transport, Clim. Dyn. 18 (2001) 71–83.
[21] A. Paul, M. Schulz, Holocene climate variability on centennial-to-millennial time scales: 2. Internal feedbacks and external forcings as possible causes, in: G. Wefer, W.H. Berger, K.-E. Behre, E. Jansen (Eds.), Climate Development and History of the North Atlantic Realm, Springer-Verlag, Berlin, 2002, pp. 55–73.
[22] M. Stuiver, P.M. Grootes, GISP2 oxygen isotope ratios, Quat. Res. 53 (2000) 277–284.
[23] D. Pollard, Ice-age simulations with a calving ice-sheet model, Quat. Res. 20 (1983) 30–48.
[24] P.U. Clark, D. Pollard, Origin of the middle Pleistocene transition by ice sheet erosion of regolith, Paleoceanography 13 (1998) 1–9.
[25] W.R. Peltier, Ice age paleotopography, Science 265 (1994) 195–201.
[26] J. Oerlemans, Model experiments on the 100 000 year glacial cycle, Nature 287 (1980) 430–432.
[27] M. Milankovitch, Mathematische Klimalehre und Astronomische Theorie der Klimaschwankungen, Handbuch der Klimalogie Band 1 Teil A, Borntraeger, Berlin, 1930, 176 pp.
[28] A. Berger, Long term variations of daily insolation and quaternary climatic changes, J. Atmos. Sci. 35 (1978) 2362–2367.
[29] E. Le Meur, P. Huybrechts, Comparison of different ways of dealing with isostasy: examples from modelling the Antarctic ice sheet during the last glacial cycle, Ann. Glaciol. 23 (1996) 309–317.
[30] H. Gallée, J.-P. van Ypersele, T. Fichefet, I. Marsiat, C. Tricot, A. Berger, Simulation of the last glacial cycle by a coupled, sectorially averaged climate-ice-sheet model: II. Response to insolation and CO_2 variation, J. Geophys. Res. 97 (1992) 15713–15740.
[31] W.H. Berger, T. Bickert, M.K. Yasuda, G. Wefer, Reconstruction of atmospheric CO_2 from the deep-sea record of Ontong Java Plateau: the Milankovitch chron, Geol. Rundsch. 85 (1996) 466–495.
[32] A. Ganopolski, S. Rahmstorf, Stability and variability of the thermohaline circulation in the past and future: a study with a coupled model of intermediate complexity, in: D. Seidov, M. Maslin, B.J. Haupt (Eds.), Oceans and Rapid Past and Future Climate Changes: North–South Connections, AGU, Washington, DC, 2001, pp. 261–275.
[33] A. Schmittner, K.J. Meissner, M. Eby, A.J. Weaver, Forcing of the deep ocean circulation in simulations of the Last Glacial Maximum, Paleoceanography 17 (2002) doi:10.1029/2001PA000633.
[34] J.-C. Duplessy, L. Labeyrie, A. Julliet-Lerclerc, J. Duprat, M. Sarnthein, Surface salinity reconstruction of the North Atlantic

Ocean during the last glacial maximum, Oceanol. Acta 14 (1991) 311–324.
[35] R.B. Alley, P.U. Clark, L.D. Keigwin, R.S. Webb, Making sense of millennial-scale climate change, in: P.U. Clark, R.S. Webb, L.D. Keigwin (Eds.), Mechanisms of Global Climate Change at Millennial Time Scales, AGU, Washington, DC, 1999, pp. 385–394.
[36] C. Wunsch, Determining paleoceanographic circulations, with emphasis on the Last Glacial Maximum, Quat. Sci. Rev. 22 (2003) 371–385.
[37] J.F. McManus, D.W. Oppo, J.L. Cullen, A 0.5-million-year record of millennial-scale climate variability in the North Atlantic, Science 283 (1999) 971–975.
[38] M. Schulz, The tempo of climate change during Dansgaard–Oeschger interstadials and its potential to affect the manifestation of the 1470-year climate cycle, Geophys. Res. Lett. 29 (2002) doi:10.1029/2001GL013277.
[39] J. Imbrie, J.Z. Imbrie, Modeling the climatic response to orbital variations, Science 207 (1980) 943–953.
[40] M.S. Poli, R.C. Thunell, D. Rio, Millennial-scale changes in North Atlantic Deep Water circulation during marine isotope stages 11 and 12: linkage to Antarctic climate, Geology 28 (2000) 807–810.
[41] C. Waelbroeck, L. Labeyrie, E. Michel, J.C. Duplessy, J.F. McManus, K. Lambeck, E. Balbon, M. Labracherie, Sea-level and deep water temperature changes derived from benthic foraminifera isotopic records, Quat. Sci. Rev. 21 (2002) 295–305.
[42] Y. Yokoyama, P. De Deckker, K. Lambeck, P. Johnston, L.K. Fifield, Sea-level at the last glacial maximum: evidence from northwestern Australia to constrain ice volumes for oxygen isotope stage 2, Palaeogeogr. Palaeoclimatol. Palaeoecol. 165 (2001) 281–297.
[43] M. Winton, The effect of cold climate upon North Atlantic deep water formation in a simple ocean–atmosphere model, J. Climatol. 8 (1997) 37–51.